Jurnal Teknologi

Full Paper

MICROSTRUCTURE AND MECHANICAL CHARACTERIZATIONS OF LM6-AL/AL_2O_3 METAL MATRIX COMPOSITES PRODUCED BY STIR CASTING TECHNIQUE

Essam R. I. Mahmoud[a]*, A. Shaharoun[a], S. Z. Khan[a], F. O. Elmahroogy[a], H. Almohamadi[b]

[a]Department of Mechanical Engineering, Islamic University of Madinah, 41411 Madinah Munawara, Saudi Arabia
[b]Department of Chemical Engineering, Islamic University of Madinah, 41411 Madinah Munawara, Saudi Arabia

Article history
Received
4 June 2021
Received in revised form
28 June 2021
Accepted
30 June 2021
Published online
20 August 2021

*Corresponding author
emahoud@iu.edu.sa

Graphical abstract

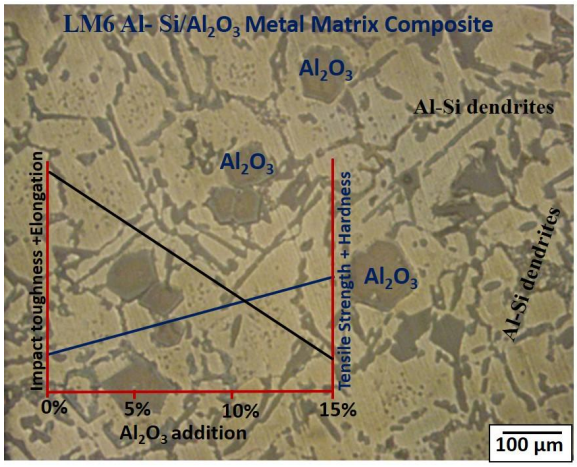

Abstract

LM6-aluminum alloy based-metal matrix composites (MMC) reinforced with Al_2O_3 ceramic particles were fabricated through stir casting. Al_2O_3 particles with different weight content (5, 10, and 15%) were dispersed into the LM6 Al-Si alloy. The macro and microstructures, mechanical properties, fracture surface, hardness, and impact toughness of the resulted MMCs together with the plain LM6 alloy were evaluated. The results showed that the added 5 wt.% Al_2O_3 was distributed homogenously with good wettability. The addition of Al_2O_3 refined the constituents of the LM6 alloy; Al-Si dendrites and the a-Al grains. At 10 wt.% Al_2O_3, some localized clusters appeared with some granular cracks. Increasing the Al_2O_3 addition to 15 wt.% resulted in particle agglomerations with multiple cracks and porosity. Both the tensile strength and the 0.2 % proof strength of the produced MMCs were improved up to 10 wt.% Al_2O_3 and then reduced. The fracture surface of 5 wt.% MMC was brittle-ductile mixed-mode fracture dominated by brittle fracture. The other percentages were almost brittle fracture. The hardness of the produced MMCs was remarkably improved. The hardness value reaches to about 86 HV at 10 wt. % Al_2O_3 addition. The impact toughness of the resulted composite materials was decreased notably at higher addition of Al_2O_3.

Keywords: Metal-matrix composites, LM6-Al-Si alloys, Stir casting, Microstructure, Mechanical properties

1.0 INTRODUCTION

LM6 Al-Si alloy is one of the most widely used casting constituents, with up to 90% of the worldwide Al castings for this alloy [1]. It has found applications in the manufacturing of marine, aerospace, aeronautical and automobile industries. Various automotive engine components such as cylinder blocks, pistons, and piston insert rings are fabricated from this alloy [2–4]. The binary system of Al-Si has a

eutectic reaction at approximately 12.3 wt% of Si at a temperature of around 577 °C. During solidification, the high value of latent heat of fusion for Si compared to Al improved castability, fluidity, and interdendritic extension; however, this also increased the solidification time [1]. The addition of Si also resulted in compromising the strength, ductility, and machinability of the Al. Near eutectic, the Al-Si alloy has ultimate tensile strength and fracture elongation of approximately in the range of 162 MPa to 168 MPa and 1.8% to 4%, respectively [2-3]. These values are significantly lower than the monolithic Al. It is generally reckoned that Al-Si alloys' mechanical properties are highly dependent on the eutectic Si, especially its morphology and homogeneity in the alloy [4]. In conventional casting, the lamellar Si in coarse grains leads to facilitate the crack formation, resulting in loss of mechanical properties. Reinforcement of various pure elements or other compounds has been studied in details to improve the mechanical behavior of Al-Si alloy [3, 5–10]. The additional phases are generally in low percentages, and the alloy commonly referred to as metal matrix composites (MMCs). Al-based MMC have application in automobile, aerospace, rail transport, marine and electrical transmission [11]. For Al-based MMCs, aluminum oxide (Al_2O_3) is one of the most preferred reinforcement materials because of the good interface affinity and non-reactive with molten Al [12]. The hardness value and the tensile strength of the Al-MMC were improved because of the reinforcement with Al_2O_3, both in low [13] and high [14] concentrations. Al_2O_3 particulates provided both grain refinement and hindered the motion of dislocation in the matrix resulted in the enhancement in the mechanical behavior of the Al-MMC [13]. For homogeneity and uniform dispersion of the additional constituents in the Al-Si alloy, numerous manufacturing and processing techniques have been introduced [7, 11, 15, 16]. These processing techniques have a direct impact on the mechanical behavior of the alloy. For example, it has been reported that 25% of the fatigue life has been improved by implementing centrifugal casting rather than gravity casting for 12 wt% Si in Al-Si alloy [7]. Traditional casting techniques have been reported to modify the processes by including additional aspects. Mold vibration has reported to marginally improve the strength and fracture elongation, subjected to the amplitude of the mold [15]. The amplitude of mold vibration has shown to have a direct effect on the fragmentation of the dendrites. There are several methods used for preparing the MMCs, such as spray formation [17], power metallurgy [18], particle infiltration technique [19], reaction techniques [20], and casting techniques [21–23]. However, MMCs manufacturing processes have inherent problems such as the formation of voids or porosity, poor wettability, non-uniform distribution of reinforcement particles. One of the feasible techniques of manufacturing MMCs that can lower such problems is the stir-casting technique [24]. The main process parameters for the stir casting are stirring temperature, time, and speed. Stir casting is a simple process having the flexibility to modify and scale-up for commercial applications without undermining the feasibility. However, the problem remains due to the wetting of reinforced particles with the molten metal and homogeneity of the particles in the matrix [23]. The homogeneity problem become severe with the high-volume fraction of the particles as well as significant density variation amongst the reinforced particles and the matrix.

This paper aims to investigate the macro and microstructure of stir cast MMCs consisted of LM6 (Al-Si alloy) as a matrix metal and reinforced with Al_2O_3. The study concentrated on the added particles homogeneity inside the matrix. Mechanical properties of the resulted composites are detailed studied.

2.0 EXPERIMENTAL WORK

In the current work, LM6 Al-Si alloy, with chemical composition listed in Table 1, was used as the matrix material. Particulate Al_2O_3 powder with a size of 44 µm (325 mesh) was used as reinforcement with three different weight percentages (5, 10, and 15 wt.%). The composite was prepared using a stir casting technique via induction melting furnace using graphite crucible. Initially, the required quantity of aluminum is heated to a temperature of 720 ± 20 °C. Afterward, the desired amount of Al_2O_3 powder was preheated to 210 °C and added slowly and gradually, followed by the stirring process. The stirring speed was around 800 rpm. The temperature was maintained to 720°C during the addition of the Al_2O_3 particles. The mixture then poured in a porcelain crucible. The cast was then cut using CNC machining for tensile test samples following the ASTM E8M-04 standard. The tensile test was conducted using a fully computerized universal tensile testing machine (Instron-3367) at a strain rate of 0.5 mm/min. For each condition, 3 specimens were prepared for the test, and the average of these values was considered. Furthermore, the tensile test fracture surface was examined using a scanning electron microscope. Microstructure observations were performed after the standard metallographic procedure using Leica optical microscope, and a scanning electron microscope (Philips XL30 ESEM environmental SEM) interfaced with Oxford Instruments INCA 250 EDS system analyzer to identify the elements of the different phases. The samples were analyzed with an X-ray diffractometer (XRD, D8 Discover with GADDS system, 35 kV, 80mA) to determine the phases formed during stir casting. The microhardness test was conducted using a Vickers microhardness tester (DVK-2 Matsuzawa Vickers Hardness). A load of 1 kg for 15 s was applied, and it was taken up to 5 readings for each condition. A standardized Charpy impact test (TQ-TE15 Impact tester) was performed

according to ASTM E23 at room temperature to obtain the amount of energy absorbed by fabricated composite during fracture. The used samples were the standard dimensions of width and thickness of 10 mm×10 mm.

Table 1 Chemical composition of the LM6 Al-Si base alloy

Element	Si	Fe	Cu	Mg	Mn	Ti	Al
Wt. %	11.2	0.6	0.2	0.1	0.5	0.2	Bal.

3.0 RESULTS AND DISCUSSION

3.1 Microstructure Analysis

The microstructure of the stir-cast plain LM6 Al-Si alloy showed normal Al-Si long dendritic structure distributed inside the α-Al phase with a grain size of approximately 80 µm in addition to many other irregular blocky intermetallics as shown in Figure 1. These long dendrite structures can be mainly attributed to the high silicon content of the matrix (11.1 wt.%), close to the eutectic composition (12.3%). The distribution of the Al-Si dendritics was almost distributed randomly, as presented in the EDS microstructure mapping of Si (green color) in Figure 1 (c). Also, these irregular blocky shapes appeared in the mapping as Mn, Fe, and Ni intermetallics constituents. These results were confirmed with point EDS analysis, as shown in Figure 2.

The different magnified microstructure of the resulted composite reinforced with 5 wt.% Al_2O_3 is shown in Figure 3. In general, the added particles were reasonably distributed inside the matrix with the absence of the clustering of particles. The reason for the uniform distribution of the reinforcement particles inside the LM6 alloy was mainly due to the stir casting technique. Also, the gradual addition of the reinforcement particles into the melt probably helped a lot in implementing the stirring process effectively and prevented the agglomeration of the particles. At the same time, there is no much difference between the density of the added Al_2O_3 particles (3.69 gm/cm^3) and that of the base LM6 Al alloy (2.65 gm/cm^3). This helps also in the better distribution of the particles in the molten metal. When there is big difference in the density between the reinforcement phase and the matrix, during melting, the heaviest element will be concentrated in the lower areas by the gravity forces, leaving the upper part with lower concentration of the reinforcement phase. At the same time, the interface between the reinforcement particles and the matrix was clean without any noticeable defect, as shown in Figure 3 (b), which also confirmed the good wettability.

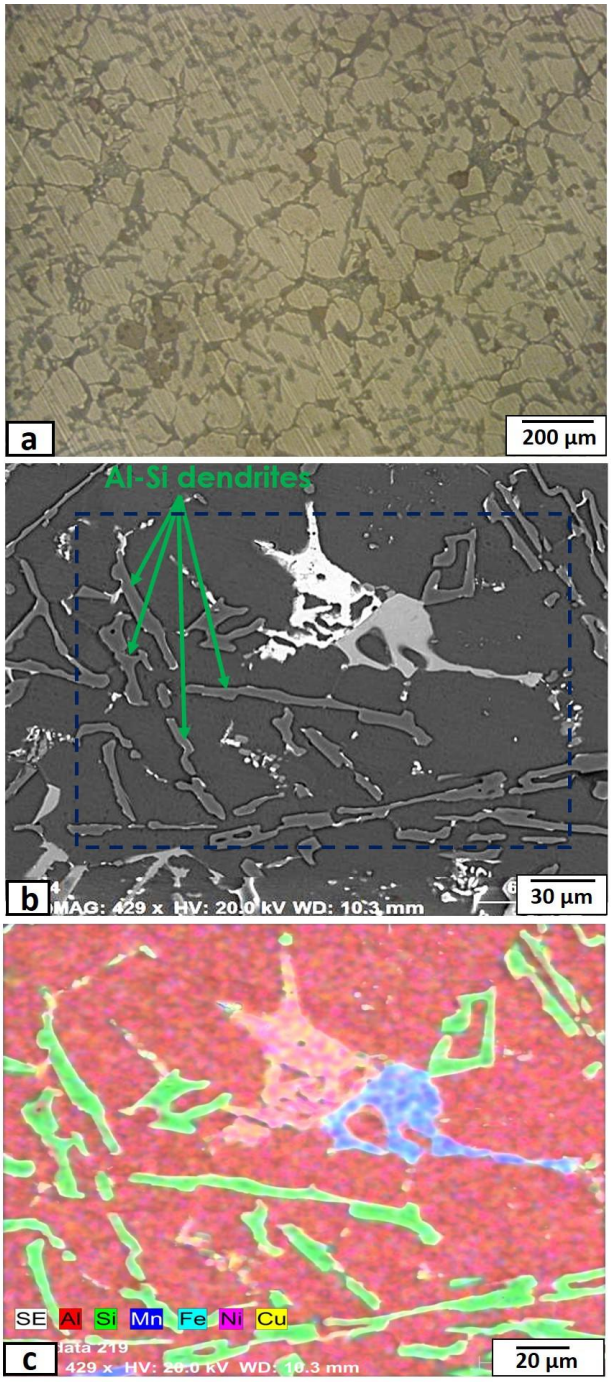

Figure 1 Micrographs of the LM6 Al-Si stir cast matrix metal, where (a) optical view, (b) SEM view and (c) EDS elemental mapping of the area shown in (b)

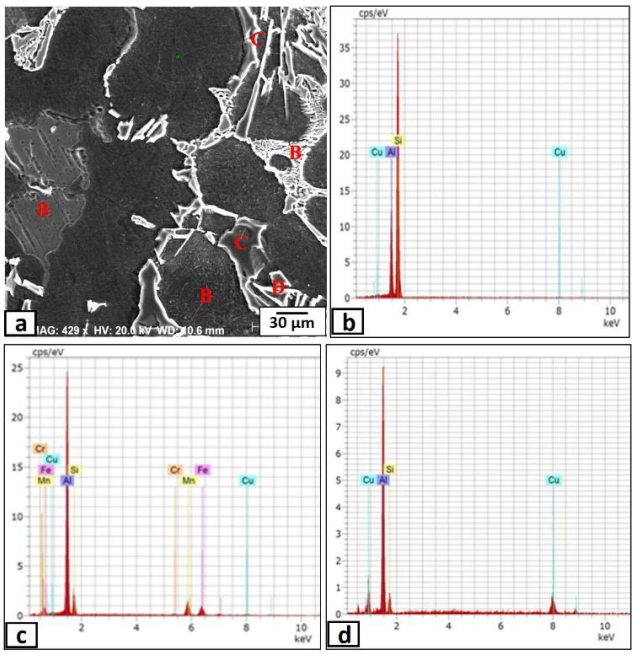

Figure 2 (a) SEM Microstructure of the LM6 Al-Si stir cast matrix metal, (b-d) Point EDS element analysis of the area shown in (a)

A good wettability may also be attributed to the preheating of the reinforcement particles before adding to the melted matrix. The addition of 5 wt.% Al_2O_3 hard particles has a significant influence on the solidification behavior of the LM6 alloy, as clearly shown in highly magnified SEM micrographs in Figure 4. The dendritic Al-Si phase became shorter and finer. The refinement mechanism of the Al-Si dendritic structure after addition of Al_2O_3 can be interpreted as follows: the Al_2O_3 particles will provide heterogeneous nucleation sites for solidification of *α*-Al phase, results in its grain refinement. The finer *α*-Al grains will limit the growing of the Al-Si dendrites by step growth mechanism [25]. Moreover, the aluminum matrix will solidify with faster cooling rates in the presence of the Al_2O_3 particles, which shared in grain refinement. To confirm that structure is for the Al-Si dendrites, the EDS mapping technique of Si (green color) was used, as shown in Figure 5. Moreover, the reinforcement addition decreased the grain size of the α-Al phase itself to its almost half size. The presence of the Al_2O_3 particles at the grain boundaries suppressed the grain growth due to the pinning effect, and hence, the size of the grains became smaller and finer [26]. The XRD pattern for the cast composites, as shown in Figure 6, revealed the presence of Al, Si eutectic and the added Al_2O_3 particles as the major peaks in addition to other intermetallics such as $CuAl_2$.

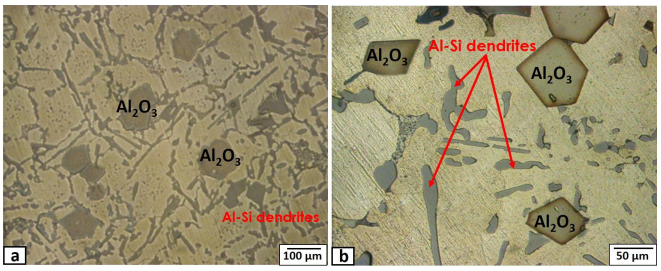

Figure 3 Different magnified optical micrographs of the produced MMC after the addition of 5 wt. % Al_2O_3

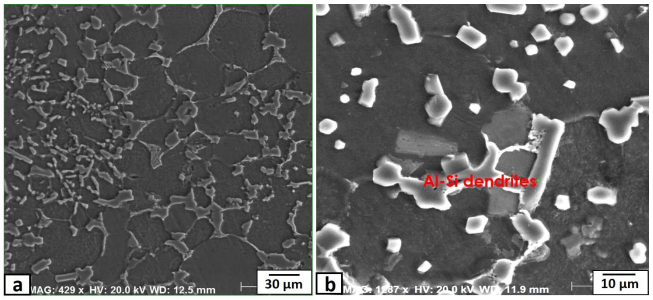

Figure 4 Different magnified SEM micrographs of the produced MMS after the addition of 5 wt. % Al_2O_3

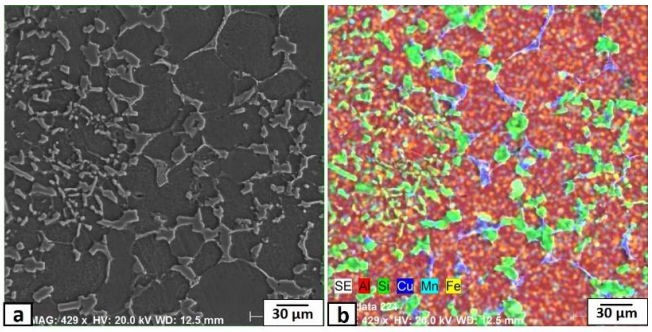

Figure 5 (a) SEM micrograph of the produced MMC after the addition of 5 wt. % Al_2O_3, and (b) EDS elemental mapping

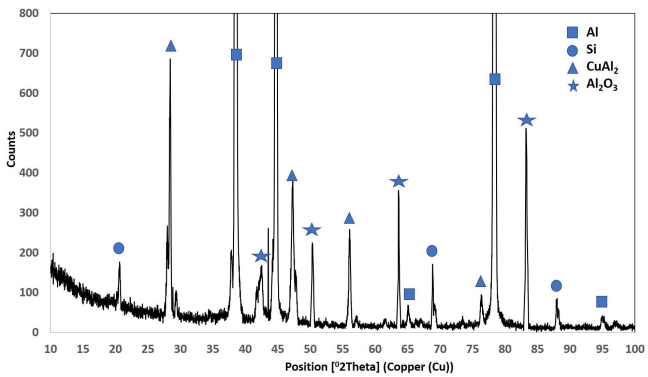

Figure 6 XRD patterns obtained from the produced MMC after the addition of 5 wt. % Al_2O_3

When the Al_2O_3 reinforcement particle addition was increased to 10 wt. %, relatively heterogeneous distribution of the particles was observed in some localized areas, as showed in Figure 7. Some Al_2O_3 particles were clustered. However, the separate particles that distributed homogenously had a good wettability with the surrounding matrix (Figure 7 (b-d)). Also, there were some crack-like defects observed around the particles in the clustered areas, as showed in Figure 7 (b). Moreover, some porosity was detected, as shown in Figure 7 (c). By increasing the addition of Al_2O_3 particles to 15 wt. %, multiple clusters and agglomerations of Al_2O_3 particles appeared, as shown in Figure 8. At the same time, many intergranular and transannular cracks were observed between the Al_2O_3 particles, in addition to porosity, as shown in Figure 8 (b-d).

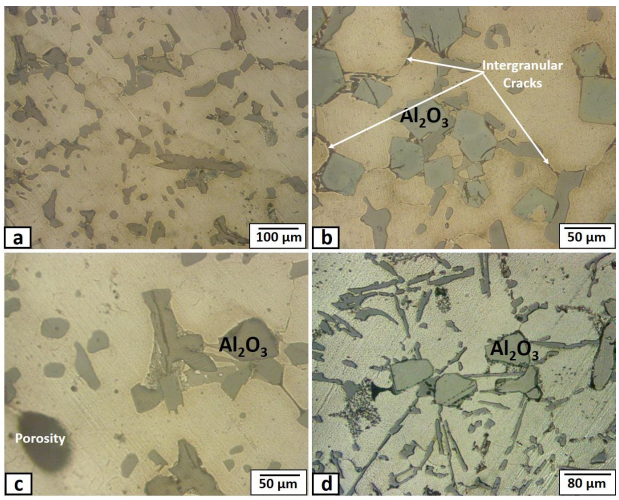

Figure 7 Different magnified optical micrographs of the produced MMC after the addition of 10 wt. % Al_2O_3

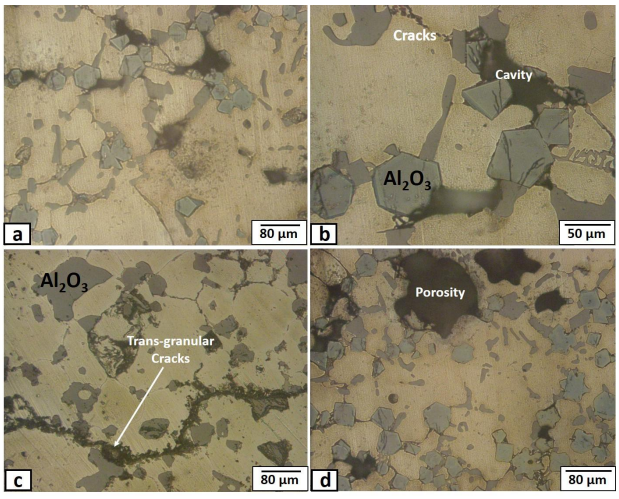

Figure 8 Different magnified optical micrographs of the produced MMC after the addition of 15 wt. % Al_2O_3

3.2 Mechanical Properties

The measured tensile test data of the LM6 alloy reinforced with 5, 10, and 15 wt. % of Al_2O_3 particles together with plain LM6 alloy matrix is presented in Figure 9. Generally, the percentage of hard Al_2O_3 particles and their distributions are the major influencing factors in evaluating the mechanical properties of the resulted composites. The ultimate tensile strength and the 0.2 % proof strength were significantly increased as the percentage of the reinforced particles increased up to 10% and then decreased. The addition of 5 wt.% Al_2O_3 particles resulted in an approximately 16% increase in proof strength and 20 % increase in ultimate tensile strength. Likewise, the addition of 10 wt.% Al_2O_3 particle resulted in a 22 % increase in proof strength and 24 % increase in ultimate tensile strength. Increasing the addition of the hard Al_2O_3 particles enhanced the load-bearing capacity and resulted in higher strength. The clean interface between the added Al_2O_3 particles and the matrix helps in load transfer from the weak matrix to the strong Al_2O_3 particles. At the same time, the dislocation loops that were created around the Al_2O_3 particles will resist the deformation during the tensile test [27]. Moreover, the matrix grain refinement done by the effect of adding Al_2O_3 particles also contributes to the strengthening of the resulted composites. When the addition of Al_2O_3 particles was 15 wt.%, the MMCs showed slightly lower values both ultimate and yield strengths. The reduction in strength could be attributed to the agglomeration and the heterogeneous distribution of Al_2O_3 particles in the matrix. Also, the formation of micro-cracks around these clustered Al_2O_3 particles considerably reduced the strength of the MMC. Regarding the ductility of the produced MMCs, the addition of Al_2O_3 particles remarkably reduced their ductility. As the content of Al_2O_3 particles increased, the elongation percentage decreased, as shown in Figure 9 (b). This could be due to the brittle nature of the ceramic Al_2O_3 particles, which led to strain hardening during deformation, thereby reducing its ductility.

The fracture surface analysis of the broken tensile test is critical and helpful in evaluating the mechanical properties of the produced MMCs. The fracture surfaces of the tensile tested specimens were observed by SEM, as shown in Figure 10. The fracture surface of the sample of 5 wt.% Al_2O_3 particles showed cleavage planes, which was the indication of major brittle fracture. At the same time, some different size dimples and cavities were observed, which suggested the presence of some ductility, as shown in Figure 10 (a). In other words, the fractured surface of the added 5 wt.% Al_2O_3 particles MMC indicated mixed-mode fracture dominated by brittle fracture. The bonding strength between the hard Al_2O_3 particles and the relatively soft Al-Si matrix is high. In this case, the fracture will be initiated in the hard Al_2O_3 particles and then transferred to the matrix. When the addition of Al_2O_3 particles was

increased to 10 wt.%, the ductile dimples got reduced, and numerous cleavage planes and tear rides were observed, as shown in Figure 10(b), which suggested almost brittle fracture. The initiation of cracks generally occurs on Al_2O_3 particles and propagates through the soft Al-Si matrix causing failure by linking up with other cracks. The sample of 15 wt. % Al_2O_3 particles (Figure 10 (c)) shows cleavage facets and tear ridges, which were the indication of a complete brittle fracture. The agglomerations and clusters of these hard Al_2O_3 particles reduced the number of isolated particles in the ductile matrix, which resulted in easy debonding of the added particles from the matrix during the tensile loading. In other words, the fracture cracks easily be propagated between the Al_2O_3 particles.

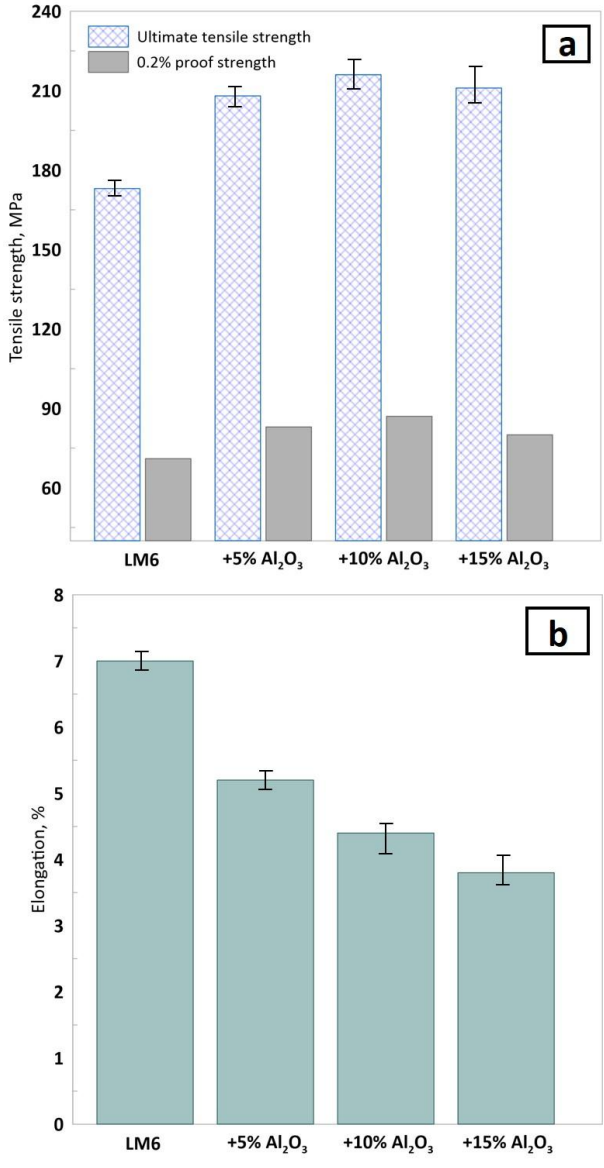

Figure 9 For all the samples evaluated, (a) Ultimate tensile strength and 0.2% proof strength, and (b) the percentage of elongation

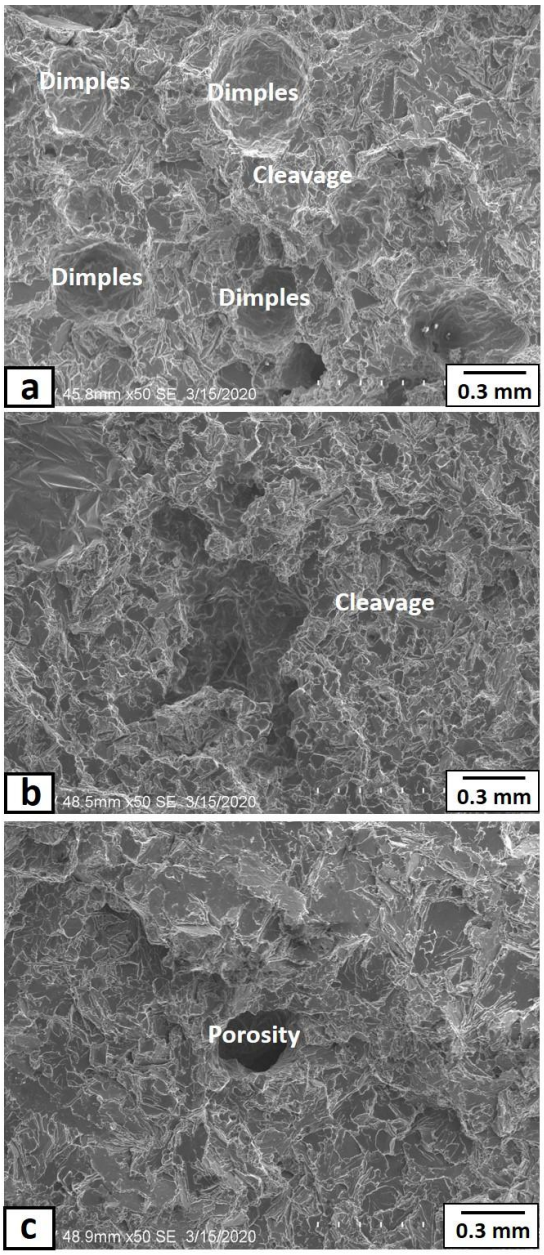

Figure 10 SEM micrographs of the tensile test fracture surfaces of the produced MMCs after the addition of Al_2O_3 (a) 5 wt. %, (b) 10 wt. %, and (c) 15 wt. %

3.3 Hardness Measurements

The readings of the hardness test indicated that there was a significant increase in the hardness value by the addition of the reinforcement phase. The hardness values were increased with increasing the percentage of the hard Al_2O_3 particles, as clearly shown in Figure 11 (a), which reached to the highest value for the 10 wt.% Al_2O_3. The loads were distributed over the hard reinforcement phase and the matrix. At the same time, grain refinement of the matrix led to an increase in the hardness of the resulted MMCs. It was observed that the sample with

15 wt.% Al_2O_3 particles showed a relatively lower increment in hardness due to the non-uniform distribution of Al_2O_3 particles. The hardness of the resulted MMCs rose by an amount of 53% when the added Al_2O_3 particles were 10 wt.%.

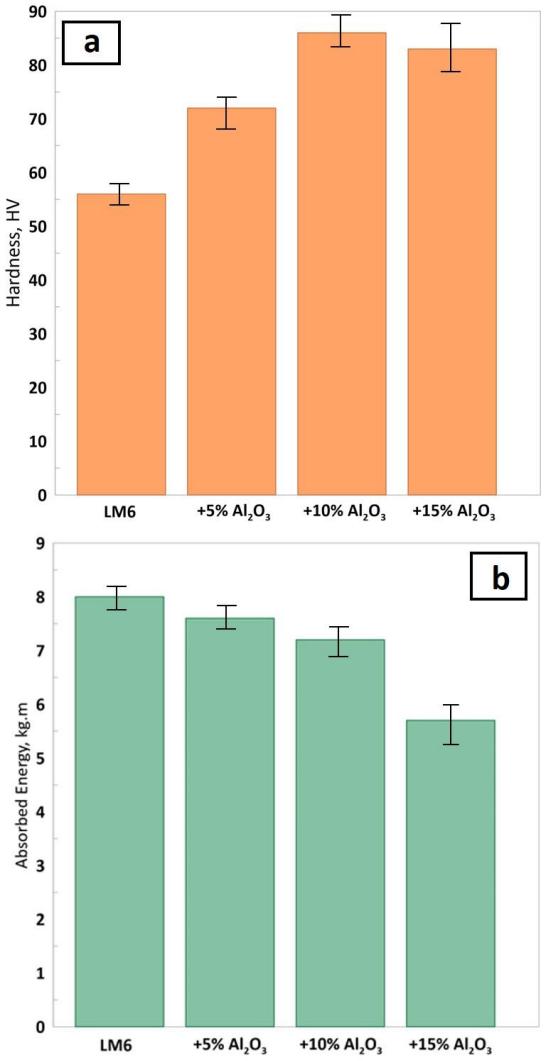

Figure 11 Vickers hardness (a) and Charpy impact toughness (b) values for all the samples evaluated

3.4 Toughness Measurements

The Charpy impact tests were conducted on the fabricated MMCs together with the plain Al-Si alloy to determine the amount of energy absorbed during fracture, and the results are shown in Figure 11(b). The plain Al-Si alloy showed the maximum impact toughness, and it decreased with the increment in the addition of hard Al_2O_3 particles. It also appeared that the sample of 5 wt.% Al_2O_3 particles to be closely related to the plain matrix Al-Si alloy being tested in this study. The reduction of the impact toughness was smooth and gradually up to 10 wt.% Al_2O_3 particles. After that, a drastic reduction was recorded at a sample of 15 wt.% Al_2O_3 particles. Generally, the impact toughness of the MMC depends on the type of the reinforcement phase, their homogeneity, and their interfacial bonding with the matrix. The added Al_2O_3 particles have extreme hardness, which increased the brittleness of the produced MMCs. Moreover, the heterogeneous distribution of the added hard particles adversely affected the impact toughness for the sample of 15 wt.% Al_2O_3 particles.

4.0 CONCLUSION

In this work, a study has been carried out to improve the mechanical properties of the LM6 Al-Si alloy by dispersing it with different percentages of Al2O3 particles to form metal matrix composites through stir casting technique. The detailed macro and microstructures, mechanical properties, hardness, and impact toughness of the produced MMCs and matrix alone were evaluated. The results of this study led to the successful fabrication of LM6 Al-Si alloy MMCs reinforced with Al2O3 particles by stir casting technique. The stir-cast plain matrix LM6 Al-Si alloy showed normal Al-Si long dendritic structure distributed inside a -Al phase with a grain size of approximately 80 µm in addition to many other irregular blocky intermetallics. The added Al2O3 particles were homogeneously distributed with the matrix at 5 wt.%, while it tended to be clustered when the addition was more than 10 wt.% of the particles. The ultimate tensile strength, 0.2 % proof strength, and hardness were improved with the increment of the content of Al2O3 particles in the matrix up to 10 wt.%, while the ductility and impact toughness showed reverse results, especially at 15 wt.%. The improvement in ultimate tensile strength and the 0.2% proof strength reached 24% and 22%, respectively, while it reached 53% in the hardness when the added Al2O3 particles were 10 wt.%. The fracture surface of the tensile test showed an almost brittle fracture, with an exception for the 5 wt.% sample; the fracture showed a few dimples of ductile fracture during fractography.

Acknowledgement

The authors would like to express their appreciation for the support provided by the Scientific Research Deanship, Islamic University of Madinah, with grant number 41/40 (Takamul 10).

References

[1] F. C. R. Hernandez, J. M. H. Ramírez, R.Mackay. 2017. Al-Si Alloys: Automotive, Aeronautical, and Aerospace Applications. Springer International Publishing. https://doi.org/10.1007/978-3-319-58380-8.

[2] H. Liao, Y. Sun, G. Sun. 2002. Correlation between Mechanical Properties and Amount of Dendritic a-Al Phase in As-cast Near-eutectic Al–11.6% Si Alloys Modified

with Strontium. *Materials Science and Engineering: A Materials Science and Engineering:* A. 335(1): PP.62-66. https://doi.org/10.1016/S0921-5093(01)01949-9.

[3] Z. Hu, X. Ruan, H. Yan. 2015. Effects of Neodymium Addition on Microstructure and Mechanical Properties of Near-eutectic Al–12Si Alloys. *Transactions of Nonferrous Metals Society of China.* 25(12): 3877-3885. https://doi.org/10.1016/S1003-6326(15)64035-3.

[4] S. D. McDonald, K. Nogita, A. K. Dahle. 2004. Eutectic Nucleation in Al–Si Alloys. *Acta Materialia.* 52(14): 4273-4280. https://doi.org/10.1016/j.actamat.2004.05.043.

[5] A. S. Zhilin, V. R. Li Jianguo, D. S. Varlamenko, V. A. Bykov. 2019. Metallography of Al-Si Alloys with Alloying by Fe up to 1%. *KnE Engineering*. 300-303. https://doi.org/10.18502/keg.v1i1.4424.

[6] S. Hegde, K. N. Prabhu. 2008. Modification of Eutectic Silicon in Al–Si Alloys. *Journal of Materials Science.* 43(9): 3009-3027, https://doi.org/10.1007/s10853-008-2505-5.

[7] G. Chirita, M. Chirita, D. Soares, F. S. Silva. 2012. Market Opportunity of Some Aluminium Silicon Alloys Materials through Changing the Casting Process. *Economics and Applied Informatics*. 2: 83-88,

[8] M. Zeren, E. Karakulak, S. Gümüş. 2011. Influence of Cu Addition on Microstructure and Hardness of Near-eutectic Al-Si-xCu-alloys. *Transactions of Nonferrous Metals Society of China.* 21(8):1698-1702. https://doi.org/10.1016/S1003-6326(11)60917-5.

[9] A. V. Pozdniakov, M. V. Glavatskikh, S. V. Makhov, V. I. Napalkov. 2014. The Synthesis of Novel Powder Master Alloys for the Modification of Primary and Eutectic Silicon Crystals. *Materials Letters.* 128: 325-328. https://doi.org/10.1016/j.matlet.2014.04.068.

[10] J. H. Ghazi. 2013. Influence of Ceramic Particles Reinforcement on Some Mechanical Properties of AA 6061 Aluminium Alloy. *Engineering and Technology Journal.* 31Part (A): 2611-2618.

[11] P. Garg, A. Jamwal, D. Kumar, K. K. Sadasivuni, C. M. Hussain, P. Gupta. 2019. Advance Research Progresses in Aluminium Matrix Composites: Manufacturing & Applications. Journal *of Materials Research and Technology*. 8(5): 4924-4939. https://doi.org/10.1016/j.jmrt.2019.06.028.

[12] G. Pilania, R. G. Hoagland, S. M. Valone. X. Y. Liu, B. J. Thijsse, I. LaziÄ. 2014. Revisiting the Al/Al2O3 Interface: Coherent Interfaces and Misfit Accommodation. *Scientific Reports*. 4. https://doi.org/10.1038/srep04485.

[13] S. A. Sajjadi, H. R. Ezatpour, M. T. Parizi. 2012. Comparison of Microstructure and Mechanical Properties of A356 Aluminum alloy/Al2O3 Composites Fabricated by Stir and Compo-casting Processes. *Materials & Design*. 34: 106-111. https://doi.org/10.1016/j.matdes.2011.07.037.

[14] M. Kok. 2005. Production and Mechanical Properties of Al2O3 Particle-reinforced 2024 Aluminium Alloy Composites. *Journal of Materials Processing Technology*. 161(3): 381-387. https://doi.org/10.1016/j.jmatprotec.2004.07.068.

[15] N. Abu-Dheir, M. Khraisheh, K. Saito, A. Male. 2005. Silicon Morphology Modification in the Eutectic Al–Si Alloy using Mechanical Mold Vibration. *Materials Science and Engineering: A Materials Science and Engineering:* A. 393(1): 109-117. https://doi.org/10.1016/j.msea.2004.09.038.

[16] P. Zhang, W. Zhang, Y. Du, Y. Wang. 2020. High-performance Al-1.5 wt% Si-Al2O3 Composite by Vortex-free High-speed Stir Casting. *Journal of Manufacturing Processes*. 56: 1126-1135. https://doi.org/10.1016/j.jmapro.2020.06.016.

[17] K. Raju, S. N. Ojha, A. P. Harsha. 2008. Spray Forming of Aluminum Alloys and Its Composites: An Overview. *Journal of Materials Science.* 43(8): 2509-2521. https://doi.org/10.1007/s10853-008-2464-x.

[18] J. M. *Torralba,* C. E. da Costa, F. Velasco. 2003. P/M Aluminum Matrix Composites: An Overview. *Journal of Materials Processing Technology.* 133(1): 203-206, https://doi.org/10.1016/S0924-0136(02)00234-0.

[19] M. K. Aghajanian, M. A. Rocazella, J. T. Burke, S. D. Keck. 1991. The Fabrication of Metal Matrix Composites by a Pressureless Infiltration Technique. *Journal of Materials Science*. 26(2): 447-454. https://doi.org/10.1007/BF00576541

[20] X. Du, T. Gao, G. Liu, X. Liu. 2017. In Situ Synthesizing SiC Particles and Its Strengthening Effect on an Al–Si–Cu–Ni–Mg Piston Alloy. *Journal of Alloys and Compounds.* 695:1-8. https://doi.org/10.1016/j.jallcom.2016.10.170.

[21] J. Zhu, W. Jiang, G. Li, F. Guan, Y. Yu, Z. Fan. 2020. Microstructure and Mechanical Properties of SiCnp/Al6082 Aluminum Matrix Composites Prepared by Squeeze Casting Combined with Stir Casting. *Journal of Materials Processing Technology*. 283: 116699. https://doi.org/10.1016/j.jmatprotec.2020.116699.

[22] G. Mc, P. Hiremath, M. Shettar, S. Sharma, U. S. Rao. 2020. Experimental Validity on the Casting Characteristics of Stir Cast Aluminium Composites. *Journal of Materials Research and Technology*. 9(3): 3340-3347. https://doi.org/10.1016/j.jmrt.2020.01.028.

[23] V. K. Annigeri. 2017. Method of Stir Casting of Aluminum Metal Matrix Composites: A Review. *Materials Today: Proceedings.* 4(2) Part A: 1140-1146, https://doi.org/10.1016/j.matpr.2017.01.130.

[24] A. Ramanathan, P. K. Krishnan, R. Muraliraja. 2019. A Review on the Production of Metal Matrix Composites Through Stir Casting – Furnace Design, Properties, Challenges, and Research Opportunities. *Journal of Manufacturing Processes*. 42: 213-245. https://doi.org/10.1016/j.jmapro.2019.04.017.

[25] R. Ding, Y. Zhao, R. Tao, Z. Zhao, L. Liang, J. Wu, X. Kai, M. Wang. 2019. Effects of Sr Addition on the Microstructures and Mechanical Properties of In-situ ZrB_2 Nanoparticles Reinforced AlSi9Cu3 Composites. *Progress in Natural Science: Materials International.* 29(5): 561-568. https://doi.org/10.1016/j.pnsc.2019.06.001.

[26] S. R. Prabhu, A. K. Shettigar, M. A. Herbert, S. S. Rao. 2019. Microstructure and Mechanical Properties of Rutile-reinforced AA6061 Matrix Composites Produced via Stir Casting Process. *Transactions of Nonferrous Metals Society of China.* 29(11): 2229-2236. https://doi.org/10.1016/S1003-6326(19)65152-6.

[27] R. Raji, S. Jannet, S. Reji, C. S. Glen. 2020. Analysis of Mechanical and Wear Properties of Al2O3 + SiC + B4C/AA5083 Hybrid Metal Matrix Composite Done by Stir Casting Route. *Materials Today: Proceedings.* 26(2): 1626-1630. https://doi.org/10.1016/j.matpr.2020.02.340.